crystals

MDPI

Article

The Role of Chemical Substitutions on Bi-2212 Superconductors

Riccardo Cabassi [1,*], Davide Delmonte [1], Muna Mousa Abbas [2], Ali Razzak Abdulridha [3] and Edmondo Gilioli [1]

[1] Istituto dei Materiali per Elettronica e Magnetismo-CNR, Parco Area delle Scienze 37/A, 43124 Parma, Italy; davide.delmonte@imem.cnr.it (D.D.); edi.gilioli@gmail.com (E.G.)
[2] Department of Radiology Techniques, Al-Hadi University College, 10011 Baghdad, Iraq; muna_moussa@yahoo.com
[3] Department of Physics, College of Education for Pure Sciences, Babylon University, 11702 Babylon, Iraq; ali_rzzq@yahoo.com
* Correspondence: riccardo.cabassi@cnr.it

Received: 7 April 2020; Accepted: 22 May 2020; Published: 1 June 2020

Abstract: We present a study on the correlation of the superconducting critical temperature (T*c*) and structural morphology with a chemically substituted high-temperature superconductor (HTS) (Bi,Pb)-2212 via Powder X-ray Diffraction (PXRD), Scanning Electron Microscopy (SEM), Energy Dispersive X-ray Spectroscopy (EDX), and *dc* magnetometry. The elements Zn, Y, Ti, and Nd are incorporated within the bismuth cuprate structure at amounts that extend the ranges currently found in literature.

Keywords: high-temperature superconductors; bismuth-based cuprates; Bi-2212

1. Introduction

Bismuth-based cuprates (BSCCO) were the first discovered high-temperature superconducting materials with no rare earth content [1]. Their crystal structure is formed by superconducting CuO_2 planes separated by charge reservoir layers crystallizing according to the general formula $Bi_2Sr_2Ca_{(n-1)}Cu_nO_{(2n+4+\delta)}$, where n is the number of CuO_2 planes in the unit cell. The superconducting phases occur at $n = 1$ (Bi-2201, T*c* = 10 K), $n = 2$ (Bi-2212, T*c* = 85 K), and $n = 3$ (Bi-2223, T*c* = 110 K). While the highest T*c* value pertains to Bi-2223, the most studied phase is Bi-2212 because of its higher thermodynamic stability and easier production route [2].

The superconducting properties of BSCCO systems—similarly to the other high-temperature superconductor (HTS) cuprates—depend on the charge-carrier concentration in the CuO_2 planes, which in turn is strongly affected by off-stoichiometricity. In particular, between oxygen excess and cationic disorder, the latter plays a dominant role [3]. With regard to this, it should be remarked that exact stoichiometries are extremely difficult to obtain in bulk compounds since, along with the starting composition, the sintering and processing conditions may affect the formation and amount of extra phases [4] or members of the homologous series with higher n values among the final results. Besides, an analysis of the ionic radii sizes shows that replacement of Ca,Sr with Pb,Cu is possible in presence of Cu^+ ions, with suitable δ values to preserve charge balance. Pb doping has been found long since [5] to yield favorable improvements: substituting Bi^{3+} with Pb^{2+} increases the formal Cu valency and thus the number of hole charge carriers [6], as a result, one has a sizable increase in the critical current $J_c(H)$ under magnetic field at optimal Pb content x = 0.16 with no significant variation in T*c* [7]. For this reason, most of the currently produced BSCCO compounds belong to the Pb-doped family (Bi,Pb)-2212, and much research effort is aimed at finding other substitutions in search of further improvements.

In this study, we investigate the effect on the superconducting and structural/morphological properties of Zn, Y, Ti, and Nd substitutions in (Bi,Pb)-2212 up to high dopant concentrations. Whilst to the best of our knowledge, there are no studies reporting on the yttrium substitutions in (Bi,Pb)-2212, earlier studies on Zn-, Ti-, and Nd-substituted (Bi,Pb)-2212 are available for concentrations up to 0.04 [8], 0.15 [9], and 0.50 [10], respectively. In this work, we extend the investigated values to 0.32, 0.67, and 0.67.

2. Results

2.1. EDX

We analyzed (Bi,Pb)-2212 samples with increasing concentrations of Zn, Y Nd, Ti, and the undoped reference sample. The chemical compositions have been obtained from the Energy Dispersive X-ray Spectroscopy (EDX) spectra shown in Figure 1. The spectra were collected in the energy range 0–40 KeV, nonetheless, no interesting features appeared above 20 KeV. The elemental contents per formula unit are reported in Table 1. In the first row, the composition of the undoped parent compound, named X000, is reported and taken as a reference; while in the following rows, the doping element of each sample is specified in the *'Dopant'* column. According to EDX analysis, the reference sample X000 has stoichiometry $Bi_{1.74}Pb_{0.39}Sr_{1.75}Ca_{0.73}Cu_{2.39}O_{7.87}$, therefore it belongs to the 2212 phase $Bi_{(2-y)}Pb_ySr_2CaCu_2O_{(8+\delta)}$, where y = 0.26 with some excess in Pb and Cu and deficiency in Sr and Ca. Assignment to the Bi-2212 phase is corroborated by the critical temperature Tc = 75 K resulting from the Zero Field Cooling (ZFC) magnetization curve that is repeated in each panel of Figure 4 for a convenient comparison with doped samples.

All the samples have similar Pb substitutions on the Bi site, apart from sample Nd05 however, which is not superconductive (see below). Moreover, the off-stoichiometry of the other cations is of the same type as for the sample X000, apart from the Ti-doped samples. On the basis of the available data, it is difficult to further speculate on the site location of each substitution.

Table 1. Formula unit elemental composition of the analyzed samples according to Energy Dispersive X-ray Spectroscopy (EDX) analysis and corresponding critical temperature Tc determined as the diamagnetic onset. The Tc value marked with *'?'* is of uncertain determination because of the low intensity of the diamagnetic signal. The *'Mass'* column refers to the samples measured with the SQUID magnetometer.

Specimen	Mass	Element							Tc (K)	
	(mg)	Bi	Pb	Sr	Ca	Cu	Dopant		2212	2223
X000	32.4	1.74	0.39	1.75	0.73	2.39	-	-	79	
Zn01	114.6	1.68	0.38	1.70	0.74	2.42	Zn	0.09	75	
Zn05	34.6	1.65	0.35	1.62	0.81	2.25	Zn	0.32	71	100?
Y01	68.2	1.81	0.16	1.78	0.91	2.16	Y	0.18	102	
Y05	62.9	1.62	0.27	1.62	0.90	1.95	Y	0.64	79	
Ti01	79.8	1.86	0.30	1.69	0.99	2.07	Ti	0.08	65	108
Ti05	89.7	1.86	0.23	1.72	0.95	1.92	Ti	0.32	65	108
Ti10	72.2	1.63	0.27	1.75	0.81	1.88	Ti	0.67	65	104
Nd01	60.5	1.63	0.26	1.79	0.76	2.41	Nd	0.17	82	
Nd05	32.0	1.41	0.04	1.76	0.88	2.25	Nd	0.67	-	
Nd10	71.4	1.42	0.29	1.60	0.85	2.17	Nd	0.67	-	

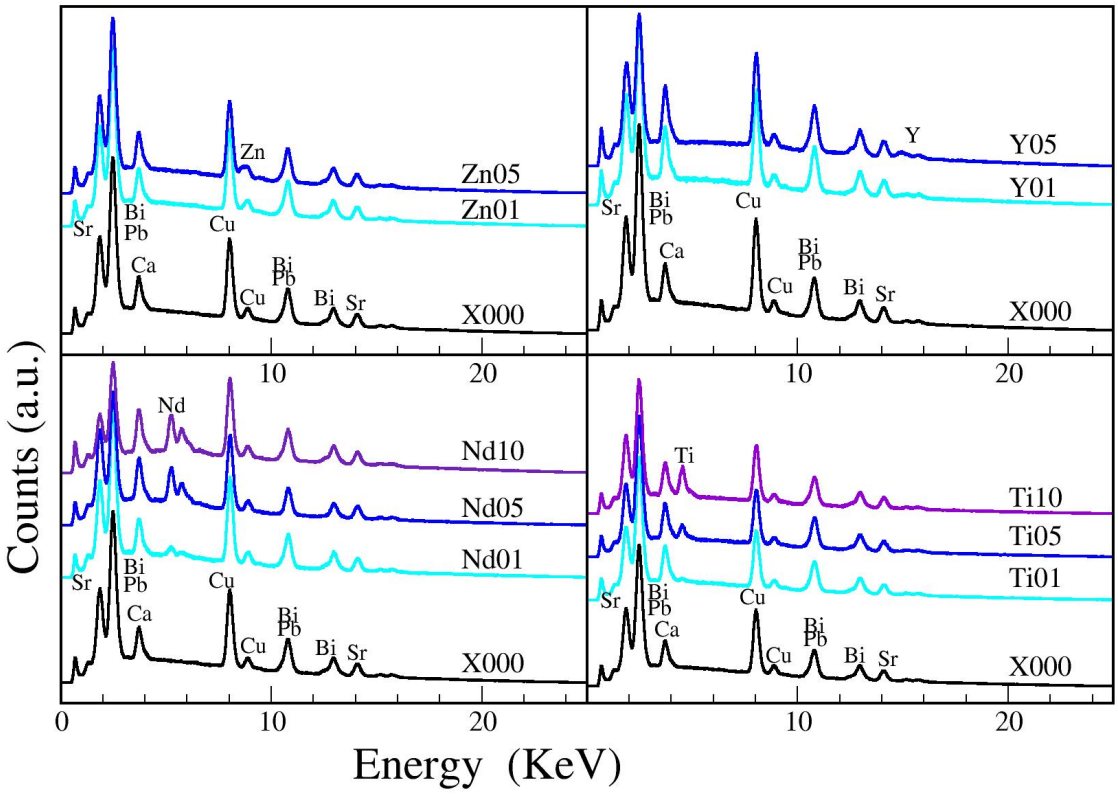

Figure 1. EDX patterns for the analyzed samples. From top to bottom: Y, Zn, Ti, and Nd substitutions. In each panel, the black line is the pattern of the reference undoped sample X000. An enlarged view of this figure, with detailed type of each emission line, is available as Figure S1 in Supplementary Materials.

2.2. PXRD

The quality of the products was also investigated by powder X-Ray diffraction (PXRD). The collected pattern of the reference sample X000 (black curve of Figure 2) matches the orthorhombic of the Bi-2212 phase (ICDD entry N.00-082-2278). A little amount of CuO is detected as the main spurious phase in all the patterns; this could explain the slight lack in composition detected for Cu by Energy Dispersive X-ray Spectroscopy (EDX) characterization. There are other traces of spurious peaks that are difficult to unambiguously address.

The Y and Zn series (see upper panels of Figure 2) do not affect the main phase stability, suggesting that Y and Zn easily substitute Ca—at least up to 0.5 in composition—within the structure. On the other hand, samples with the higher concentration of Nd and Ti ($x \simeq 0.5$–1) start to degrade the Bi-2212 phase, forming traces of spurious compounds (mixed Sr,Cu oxides). Interestingly, for Nd-substitution, the Bi-2212 phase is no longer superconducting for Nd ≥ 0.5, while in the case of Ti—in particular Ti10—the formation of higher member Bi-2223 phase was observed, in agreement with the double Tc onset detected (Figure 4c)—the latter in the temperature range 104–108 K.

The effect of a heavy Y- and Nd-doping clearly leads to a large contraction of the cell along the (0 0 10) c-axis (much larger than for Zn and Ti); reversely, the b-axis slightly enlarges, more significantly for Nd than for Y substitutions, as shown in the PXRD patterns zoomed in the 2θ region 27–34.5°, where the most intense and significative peaks are located for Y05, Nd05, and the reference sample X000 (Figure S3 in Supplementary Materials).

The simple one-to-one correlation between the crystallographic axes and the transition temperature Tc does not account for the complexity of the HTS cuprates. Since their discovery, a massive experimental and theoretical effort has been focused to find which interatomic distances within the unit cell affect the superconductivity, with particular attention to the CuO_2 planes aligned

along the c-axis of the highly anisotropic HTS cell, where the superconductivity actually takes place. The number, distance, and interlayer coupling of the CuO_2 planes, their inner structure, *buckling angle*, in-plane cationic disorder, and the relation with the nonsuperconducting spacers were modified via cationic substitution. Despite the extensive work, the experimental results are still contradictory. In our case, the contraction of the c-axis of the heavily doped BSCCO samples is associated to the disappearance of the superconductivity in the Nd05 samples, and the drastic drop of the superconducting fraction in the Y05 one.

2.3. SEM Morphology

The surface morphologies observed by Scanning Electron Microscopy (SEM) images are reported in Figure 3. The reference sample features platelet-like grains of size in the order 10 μ, clearly depending on the synthesis/sintering procedures. The effect of doping on morphologies is of two opposite types, depending on the dopant element.

Moderate doping with Zn or Ti increases the size of platelets. Higher concentration of Ti, as in sample Ti10, induces a remarkably compact structure formed by merged layers and crossed by just few tubular cavities. Platelets' surface are clean, smooth, and the borders are neat.

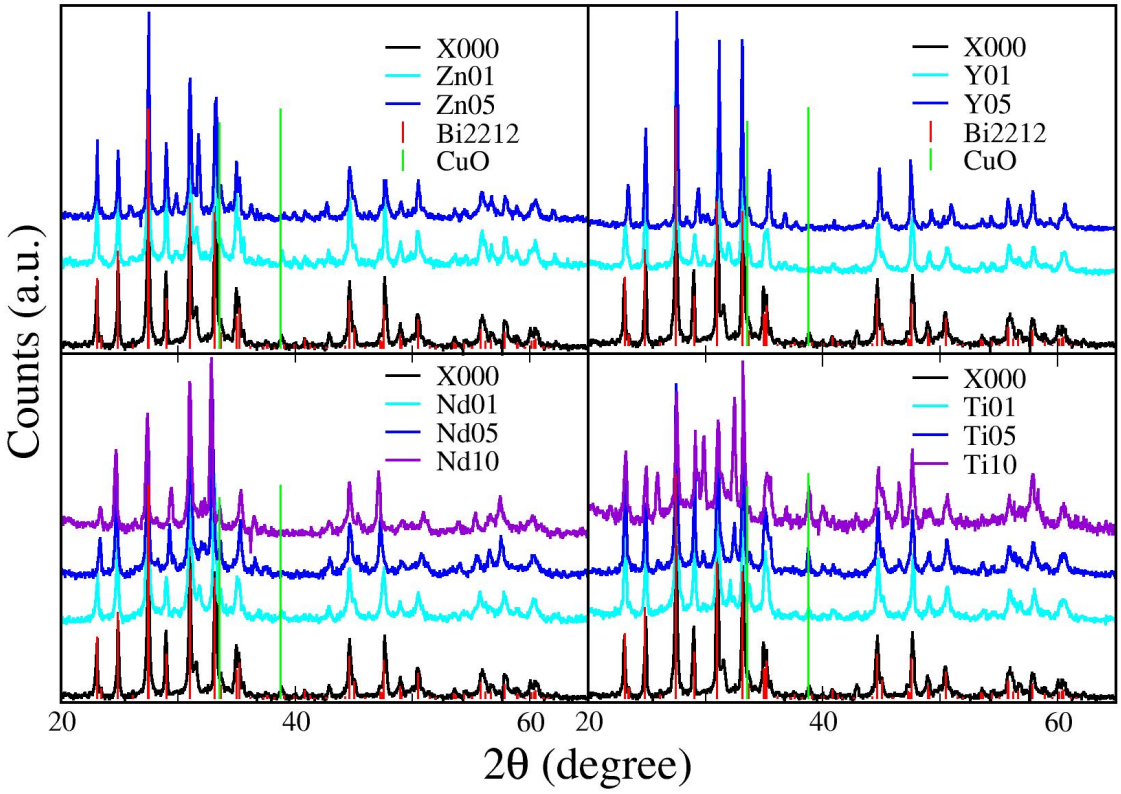

Figure 2. Powder X-ray Diffraction (PXRD) patterns for the analyzed samples. From top to bottom: Y, Zn, Ti, and Nd substitutions. In each panel, the black line is the pattern of the reference undoped sample. Red bars: Bi-2212 pattern from ICDD (chart n.00-082-2278). Green bars: CuO impurity pattern. An enlarged view of this figure is available as Figure S2 in Supplementary Materials.

On the contrary, samples with Y and Nd show smaller flat flakes in the order of ∼2 µm, with size decreasing on increasing the dopant content and approaching a granular aspect ratio for sample Y05. Similar trends in the evolution of morphology have already been observed with other dopant species [11].

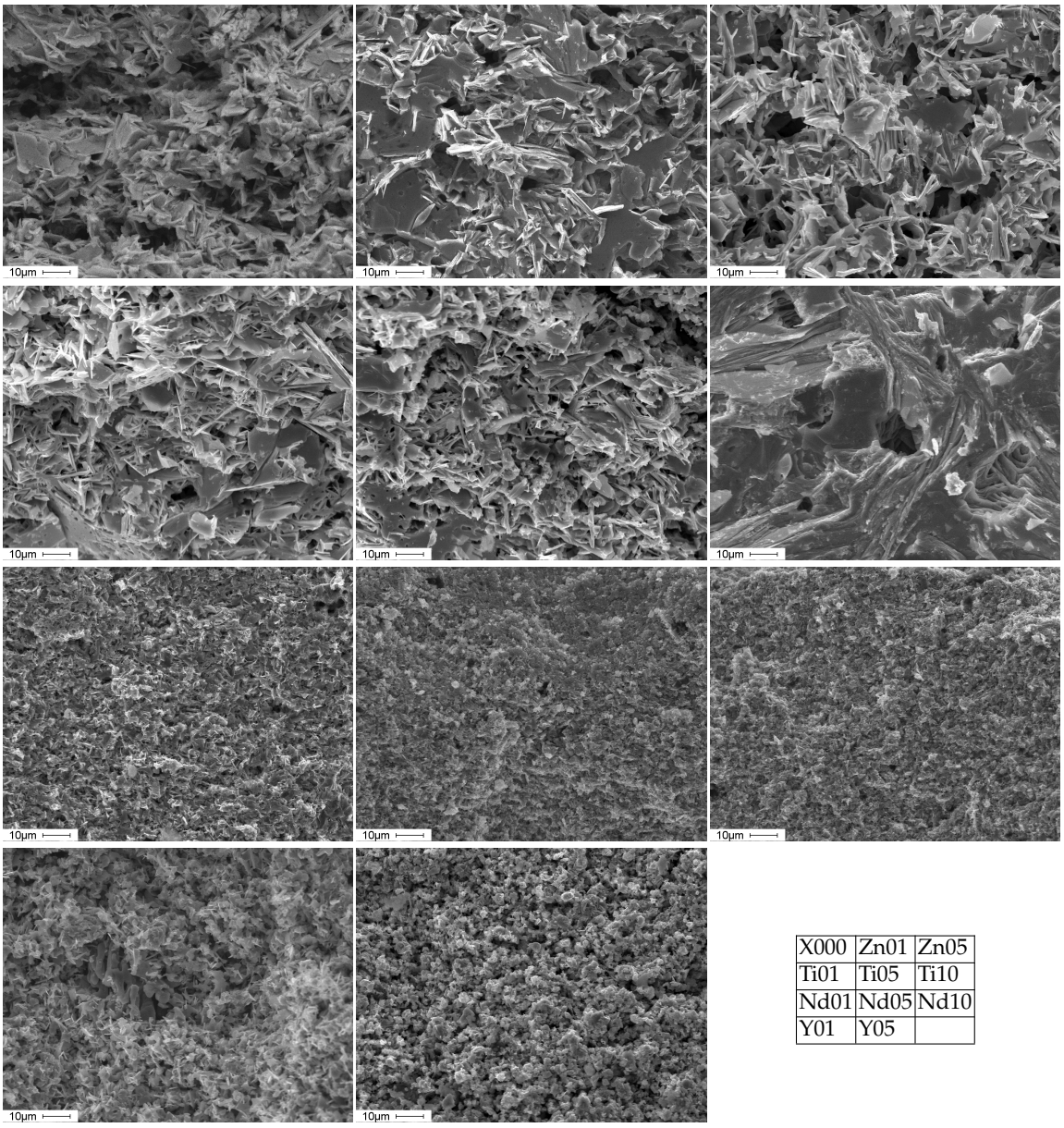

Figure 3. SEM surface micrographs of samples. From left to right, top to bottom: X000, Zn01, Zn05, Ti01, Ti05, Ti10, Nd01, Nd05, Nd10, Y01, Y05, as depicted in lower right corner.

2.4. Magnetic Characterization

In Figure 4, the resulting M(T) curves for reference and substituted samples are displayed. It is worth recalling that in a perfectly diamagnetic sample, the measured magnetic susceptibility is

$$\chi = \frac{-1}{4\pi(1-N)}, \tag{1}$$

where N is the demagnetizing factor along the magnetization direction. It is easy to realize that N plays an important role on the absolute value of the measured signal in superconducting materials. For example, two cylinders with aspect ratio height/diameter equal to 1 and 2 have demagnetizing factors 0.232 and 0.069, respectively [12]: substituting into Equation (1), one obtains a difference between the measured susceptibilities amounting to a remarkable 30%. Considering that our samples had different and irregular shapes, a rigorous quantitative comparison of their diamagnetic intensities would be of little meaning. Therefore, the numerical value of diamagnetic intensities will be taken into

account only in case of very notable differences between the samples, as in the case of Y substitutions. We will rather focus on estimating the critical temperatures T*c* that, in the M(T) curves, can be identified with the temperature of the diamagnetic onset.

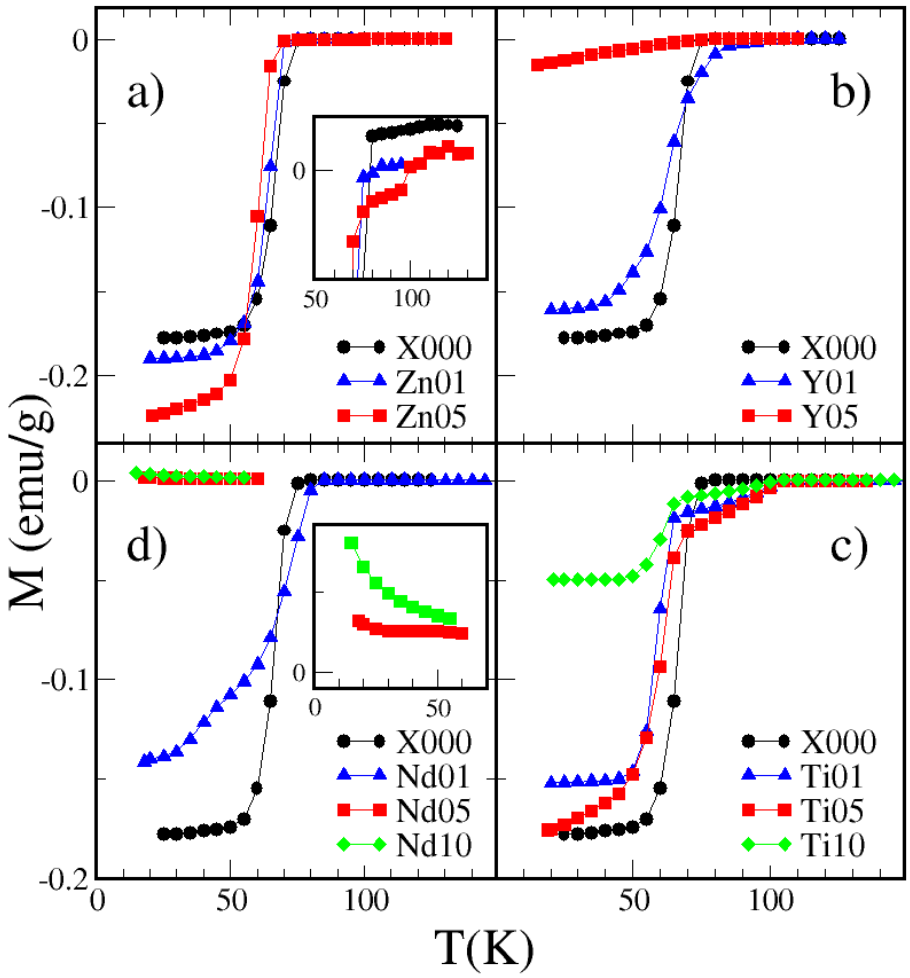

Figure 4. Zero Field Cooling (ZFC) magnetization curves of doped samples measured in applied magnetic field H = 100 Oe. X000 reference sample is also shown in each panel for comparison. Panels clockwise from top left: (**a**) Zn, (**b**) Y, (**c**) Ti, and (**d**) Nd substitutions. Inset of panel (**a**): magnified vision highlighting the diamagnetic signal above T*c* of the Bi-2212 phase, suggesting the presence of a small fraction of Bi-2223 phase. Inset of panel (**d**): magnified vision of the paramagnetic signal of the nonsuperconductive samples Nd05 and Nd10.

2.4.1. Nd

In Nd-doped (Bi,Pb)-2212 a replacement of Nd^{3+} for Sr^{2+} ions occurs; measuring Nd occupations per f.u. x from 0.1 to 0.5 yields an optimal value $x = 0.2$ corresponding to the highest critical temperature T*c* = 94 K. Above the optimal x value, T*c* decreases down to T*c* = 82 K for $x = 0.5$ [10]. Our Nd-doped samples comprise of a specimen with x close to the optimal value (Nd01, $x = 0.17$) and two overdoped samples with $x = 0.67$, thus extending the range analyzed in Reference [10]. As can be observed in panel (*a*) of Figure 4, sample Nd01 confirms an increase in T*c* with respect to the undoped reference specimen X000; while in the two overdoped specimens, the superconductivity is completely suppressed. It is worth noting that Nd5 and Nd10 samples show the same Nd content; such a high Nd concentration seems to partially substitute Bi and Pb (Nd05) or Bi and Sr (Nd10); in both cases, the superconductivity vanishes.

2.4.2. Y

Yttrium substitution is among the earliest attempted to achieve a Tc increase in Bi-2212, finding the best doping value x = 0.1∼0.15 with corresponding Tc∼ 92 K [13,14]; this has been attributed to the effect of Y^{3+} substituting Ca^{2+}, which compensates for the hole excess in CuO_2 planes and restores the charge carrier concentration to its optimal value. As previously mentioned, in the literature, we did not find studies on Yttrium substitutions in (Bi,Pb)-2212, nonetheless, our measurements—panel (*b*) of Figure 4—show a similar effect on (Bi,Pb)-2212: sample Y01 (x = 0.17) confirms an increase in Tc of about 20 K with respect to the undoped reference specimen X000; on the other hand, increasing Y content up to x = 0.64, as in sample Y05, the diamagnetic onset is restored to the undoped values. Moreover, the diamagnetic intensity at the lowest measured temperature drops from −0.178 emu/g of the undoped sample to −0.015 emu/g only of Y05. This fall is too important to be ascribed to the demagnetizing effect discussed in Section 2.4, as Equation (1) would lead to unrealistic demagnetizing factors, and points rather to a strong reduction of the superconductive volume fraction of the specimen. The latter feature is likely related to the weak connectivity of the granular morphology evidenced in Table 3.

2.4.3. Zn

Zn substitution is known to induce a Tc depression in both Bi-2212 [15] and (Bi,Pb)-2212 [8]. Such depression has been explored in [8] for Zn content up to x = 0.04 and results to be in the order of Δ Tc∼ 10 K. We have extended the explored range up to x = 0.32, panel (*d*) of Figure 4, finding that the Tc depression maintains approximately the same magnitude even at such great doping content. A close inspection highlights the occurrence of diamagnetic signal even in the range above Tc of the Bi-2212 phase: this suggests the possible formation of Bi-2223 phase induced by a high level of Zn doping.

2.4.4. Ti

Ti doping in the BSCCO system yields the formation of Bi-2212/2223 multiphase samples with an improving of the superconducting properties for small Ti content x, and successive worsening for further x increasing up to the highest essayed value $x = 0.15$ [9,16]. The ionic radius of Ti^{4+}(68 pm) is similar to Cu^{2+}(72 pm), so it has been suggested that the former can substitute the latter in the crystal lattice. In a similar way, our Ti-doped samples feature the emerging of the high-Tc Bi-2223 phase at the expense of the Bi-2212 phase, panel (*c*) of Figure 4. According to literature, the nominal doping values of samples Ti01 and Ti05 should induce a sizable decrease on Tc in both the Bi-2223 and Bi-2212 components [16]. On the contrary, samples Ti01 and Ti05 have the same Tc values, while in sample Ti10, the variation of Tc can be considered negligible if one takes into account the very high x value.

3. Discussion and Conclusions

In the Nd- and Y-doped samples, our results confirm the worsening of the superconducting properties with x exceeding the values usually reported. For these samples, SEM micrographs show a reduced grain size, with deterioration of connectivity. On the contrary, Zn- and Ti-doped samples feature a substantial independence in the high x range. This could be at least partially related to the different grain sizes that appear to be greater than what can be found in literature. This is true for both Zn doping [8] and even more for Ti doping, where Tc appears to be independent on x. In principle, this could suggest that the majority of the Ti ions were segregated as impurities, rather than entering the BSCCO crystal lattice. However, SEM and EDX show a uniform compositional distribution, with no evidence of substituents segregation or inhomogeneities in platelet borders and surfaces. Moreover, by comparison with the images reported in Reference [9], one can notice the greater size of platelets, even from the low doping values. The latter, likely due to the different conditions of synthesis and sintering, can probably be the true origin of the different behaviors.

In short, the main conclusions are the following:

- We have measured (Bi,Pb)-2212 samples doped with Nd, Y, Zn, and Ti with content x exceeding the values reported in literature.
- Irrespective to the amount of substitutions, Ti induces the formation of the (Bi,Pb)-2223 phase in traces, clearly visible from the corresponding Tc value.
- The substituents show uniform compositional distribution, with no evidence of segregation, but leading to different grain size and grain connectivity.
- A high degree of substitutions (mainly for Y and Nd) induces similar structural changes (large contraction of the c-axis and a shorter expansion of b), but with a negative effect on Tc that remains unchanged for Y and has a strong reduction of the superconducting fraction; while it completely vanishes for Nd.

Owing to the structural and chemical complexity of the BSCCO HTSs and in spite of the long experimental activity, this work confirms the need of detailed studies to take into account the multiple structural changes induced by different chemical substitutions of (Bi,Pb)-2223 phase, and to clarify the controversial issue of the correlation with Tc.

4. Materials and Methods

Polycrystalline samples have been prepared as reported in Reference [17], starting from stoichiometric mixture of the high-purity binary oxides which were calcined in air at 800 °C for 24 h. The powder pressed into disk-shaped pellets using a manual hydraulic press type (SPECAC) under different pressures around 0.6 GPa. The pellets were sintered in air at 835∼850 °C for 140 h. From the obtained pellets, fragments of irregular shape, and linear dimensions of ∼2 mm have been obtained and addressed to the various characterization techniques.

The phase identification was carried out by PXRD, using the Siemens D500 diffractometer, emitting CuKα_1 and CuKα_2 wavelengths (average λ = 1.54178 Å), with no filter for the CuKβ.

The surface morphology of the samples was studied using SEM (Philips 515), operating at 25 kV, and equipped with an EDX "Phoenix" detector for compositional analysis. ZFC magnetization curves M(T) have been measured in applied magnetic field H = 100 Oe using a commercial SQUID magnetometer MPMS-5T (Quantum Design Co., San Diego, CA, USA).

Supplementary Materials: The following are available online at http://www.mdpi.com/2073-4352/10/6/462/s1, Figure S1. EDX patterns for the analysed samples, Figure S2. PXRD patterns for the analysed samples, Figure S3. Expanded PXRD patterns for Y05, Nd05 and reference sample X000.

Author Contributions: Conceptualization, R.C., D.D. and E.G.; methodology, R.C., D.D. and E.G.; validation, R.C., D.D. and E.G.; formal analysis, R.C., D.D. and E.G.; resources, R.C., D.D., M.M.A., A.R.A. and E.G.; investigation, R.C., D.D., M.M.A., A.R.A. and E.G.; writing—original draft preparation, R.C.; writing—review and editing, R.C., D.D. and E.G.; visualization, R.C. All authors have read and agreed to the published version of the manuscript.

Funding: This research received no external funding.

Acknowledgments: The authors thank P. Ferro (IMEM-CNR) for PXRD, F. Pattini (IMEM-CNR) for SEM data collection and S. Rampino (IMEM-CNR) for fruitful discussion.

Conflicts of Interest: The authors declare no conflict of interest.

Abbreviations

The following abbreviations are used in this manuscript:

BSCCO	Bismuth based cuprates
EDX	Energy Dispersive X-ray Spectroscopy
HTS	High Temperature Superconductor
PXRD	Powder X-ray Diffraction
SEM	Scanning Electron Microscopy
ZFC	Zero Field Cooling

References

1. Maeda, H.; Tanaka, Y.; Fukutomi, M.; Asano, T. A new high-Tc oxide superconductor without a rare earth element. *Jpn. J. Appl. Phys.* **1988**, *27*, L209. [CrossRef]
2. Manfredotti, C.; Truccato, M.; Rinaudo, G.; Allasia, D.; Volpe, P.; Benzi, P.; Agostino, A. Annealing temperature dependence of the 2223 phase volume fraction in the Bi–Sr–Ca–Cu–O system. *Phys. C Supercond.* **2001**, *353*, 184. [CrossRef]
3. Eisaki, H.; Kaneko, N.; Feng, D.L.; Damascelli, A.; Mang, P.K.; Shen, K.M.; Shen, Z.-X.; Greven, M. Effect of chemical inhomogeneity in bismuth-based copper oxide superconductors. *Phys. Rev. B* **2004**, *69*, 064512. [CrossRef]
4. Miao, H.; Kitaguchi H.; Kumakura H.; Togano K.; Hasegawa T.; Koizumi T. J_c enhancement of Bi-2212/Ag multilayer tapes by per-annealing and intermediate rolling process. *Adv. Cryogenic Eng.* **2000**, *46*, 559.
5. Togano, K.; Kumakura, H.; Maeda, H.; Yanagisawa, E.; Takahashi, K. Properties of Pb-doped Bi-Sr-Ca-Cu-O superconductors. *Appl. Phys. Lett.* **1988**, *53*, 1329. [CrossRef]
6. Coşkun, A.; Ekicibil, A.; Özçelik, B. Superconductivity of $Bi_{1.6}Pb_{0.4}Sr_2Ca_3Cu_4O_{12}$. *Chin. Phys. Lett.* **2002**, *19*, 1863.
7. Kumar, J.; Ahluwalia, P.K.; Kishan, H.; Awana, V.P.S. Significant Improvement in Superconductivity by Substituting Pb at Bi-site in $Bi_{2-x}Pb_xSr_2CaCu_2O_8$ with x = 0.0 to 0.40. *J. Supercond. Nov. Magn.* **2010**, *23*, 493–499. [CrossRef]
8. Bouaïcha, F.; Mosbah, M.F.; Amira, A.; Ait-Kaki, A.; Boussouf, N. Effect of Zn doping in Bi (Pb)-2212 superconducting ceramics. *Phys. Stat. Sol.* **2006**, *3*, 3036. [CrossRef]
9. Hamid, N.A.; Abd-Shukor, R. Effects of TiO_2 addition on the superconducting properties of Bi-Sr-Ca-Cu-O system. *J. Mater. Sci.* **2000**, *35*, 2325. [CrossRef]
10. Biju, A.; Syamaprasad, U.; Rao, A.; Xu, J.G.; Sivakumar, K.M.; Kuo, Y.K. Structural and transport properties of Nd doped (Bi, Pb)-2212. *Phys. C Supercond.* **2007**, *466*, 69. [CrossRef]
11. Bal, S.; Dogruer, M.; Yildirim, G.; Varilci, A.; Terzioglu, C.; Zalaoglu, Y. Role of Cerium Addition on Structural and Superconducting Properties of Bi-2212 System. *J. Supercond. Novel Magnet.* **2012**, *25*, 847. [CrossRef]
12. Chen, D.; Brug, J.A. Demagnetizing factors for cylinders. *IEEE Trans. Magnet.* **1991**, *21*, 3601. [CrossRef]
13. Zavaritskî, N.V.; Zavaritskî, V.N.; Mackenzie, A.P.; Orekhov, Y.F. Effect of yttrium on the increase in T_c of Bi(2212) crystals. *JETP Lett.* **1994**, *60*, 193.
14. Özçelik, B.; Nane, O.; Sotelo, A.; Madre, M.A. Effect of Yttrium substitution on superconductivity in Bi-2212 textured rods prepared by a LFZ technique. *Ceram. Int.* **2016**, *42*, 3418–3423. [CrossRef]
15. Kuo, Y.K.; Schneider, C.W.; Skove, M.J.; Nevitt, M.V.; Tessema, G.X.; McGee, J.J. Effect of magnetic and nonmagnetic impurities (Ni, Zn) substitution for Cu in $Bi_2(SrCa)_{2+n}(Cu_{1-x}M_x)_{1+n}O_y$ whiskers. *Phys. Rev. B* **1997**, *56*, 6201. [CrossRef]
16. Lu, Y.F.; Qiu, X.L.; Chao, X.X. The effect of titanium substitution in the $Bi_{1.6}Pb_{0.4}Sr_2Ca_2Cu_{3-x}Ti_xO_{10+y}$ system. *Solid State Commun.* **1995**, *95*, 259. [CrossRef]
17. Hermiz, G.Y.; Abbass, M.M.; Gilioli, E. Superconductivity of $(Bi_{0.7}Pb_{0.3})_2Ag_xSr_2Ca_2Cu_3O_{10+\delta}(0 \leq x \leq 0.5)$. *Atti Della Fondazione Giorgio Ronchi* **2009**, *64*, 1–8.